Frascati Physics Series Vol. LIX (2014), pp. 00-00
4^{th} Young Researchers Workshop: *"Physics Challenges in the LHC Era"*
Frascati, May 12 and 15, 2014

PERFORMANCE STUDY OF MICROMEGAS MUON CHAMBERS FOR ATLAS UPGRADE

Marco Sessa
on behalf of ATLAS Micromegas Group
Università degli Studi Roma Tre & *INFN Sez. di Roma Tre*
Via della Vasca Navale 84, 00146 Roma

Abstract

The largest of the ATLAS Phase-1 upgrades of the Muon Spectrometer concerns the replacement of the first muon station of the high-rapidity region with the so called New Small Wheel (NSW), that will be installed during the next Long Shutdown in 2018. The NSW employs Micromegas (MM) and small-strip Thin Gap Cahmbers (sTGC) detectors, which will allow to reconstruct the muon momentum with a resolution better than 15% at $P_T \sim 1\ TeV$. In this paper, the performance of MM chambers and, in particular, the spatial resolution and the efficiency, obtained using data from different test beam campaings, will be described.

1 Introduction

Two long shutdowns, LS2 and LS3, are planned for the ATLAS detector, rispectively in 2018 and 2022. After LS3, the luminosity will be increased up to

$6 \div 7 \cdot 10^{34}\ cm^{-2}s^{-1}$ and the number of pile-up events will be ~ 200. Therefore, a very high rate in the forward region of the Muon Spectrometer (especially in the Small Wheel) is expected, with a resulting increase of detectors inefficiency.

The luminosity increase of the LHC will require an upgrade of the ATLAS detector, in order to keep the excellent performance of today in the new running conditions at higher energy. The forward part of the Muon Spectrometer will be replaced with the New Small Wheel (NSW), that will guarantee higher rate capabilities and a better performance for the Level-1 muon trigger. The expected rate at the ultimate luminosity of LHC is expected to be about $15\ KHz/cm^2$ on the New Small Wheel.

2 Micromegas Technology

Micromegas (MICRO MEsh GAseous Structure) chambers belong to the family of Micro Pattern Gaseous Detectors (MPGD). They consist of a planar electrode (drift cathode), a gas ($Ar : CO_2$) gap of $5\ mm$ thickness, acting as conversion and drift region, and a thin metallic mesh positioned at $128\ \mu m$ distance from the readout electrode, creating the amplification region [1]. As shown in Fig.1, charged particles, traversing the drift space, ionize the gas. The electrons, liberated by the ionization processes, drift towards the mesh (in some tens of nanoseconds) and in the thin amplification region the electron avalanche takes place ($Gain \sim 10^4$). The charge is collected by resistive strips, capacitively coupled to the read-out strips.

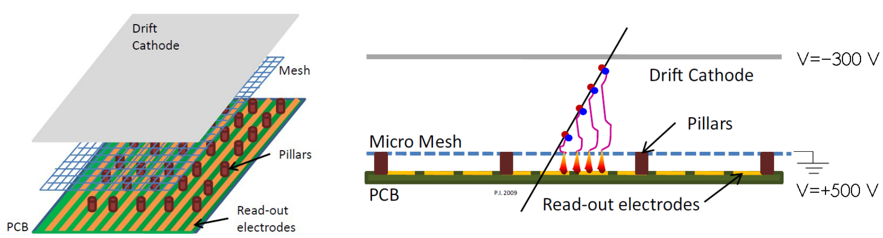

Figure 1: Layout and operating principle of a Micromegas chamber.

3 Track reconstruction

Two methods can be used to reconstruct the point of passage of a particle through the MM chamber.

3.1 Charge Centroid Method

Charge centroid method is based on "neighbouring strips alghoritm", that allows to group several fired strips into a cluster. It works very well for tracks perpendicular to the MM chamber [2]. The X coordinate is obtained using the weighted mean shown in (1):

$$X = \frac{\sum_i q_i x_i}{\sum_i q_i} \qquad (1)$$

where x_i is the strip position and q_i is the maximum value of the collected charge on that strip. The summation is extended over all strips of a specific cluster.

3.2 μTPC Method

As in the Time Projection Chambers, the μTPC method, used for impact angles larger than 10°, exploits time information in order to obtain the coordinate perpendicular to the readout plane. The drift time (t_{drift}) of the electrons, produced during the ionization processes in the drift region (5 mm thick), is obtained by a Fermi-Dirac fit of time sampled signal of each strip. In this way, using $z - t$ relation ($z = t_{drift} \times v_{drift}$), it's possible also to reconstruct a local track segment in each chamber [3]. Using the gas mixture of $Ar : CO_2$ and the voltages shown in Fig.1, the electrons drift velocity is $\sim 47\ \mu m/ns$.

4 Test Beam Data Analysis

The analysis described in this paper has been perfomed using data recorded during different test beam campaigns, in particular at CERN with $120 \div 150\ GeV$ π^- and at DESY with an e^- beam of $1 \div 6\ GeV$. Two different $10 \times 10\ cm^2$ size MM chambers prototypes have been tested:

- Tmm chambers with 250 μm strips pitch and XY readout;
- T chambers with 400 μm strips pitch and X readout.

MM chambers strips are read-out using the APV25 chips, sampling the signal every 25 ns. The test beams, indicated above, offer the possibility to study MM performance under different conditions of angle ($0° \div 40°$), magnetic fields ($0\ T \div 1\ T$) and operating voltages.

4.1 μTPC optimization

A small angular bias is observed due to capacitative induction of the signal on neighbouring strips. The effect, clearly, is more evident on the first and last strip of the cluster. This causes a small angular bias on the reconstructed tracks, as shown in Fig.2. A possible correction consists in:

- don't use first and last strip if its charge is more than 6 times smaller than its neighbour;
- correct the charge position for the edge strips of the cluster according to:

$$x_{cor}^{first} = \left(\frac{cluster_{length}}{6}\right)^2 \cdot \left(\frac{q_0}{q_1}\right) \cdot \left(\frac{pitch}{2}\right)$$
$$x_{cor}^{last} = \left(\frac{cluster_{length}}{6}\right)^2 \cdot \left(\frac{q_n}{q_{n-1}}\right) \cdot \left(\frac{pitch}{2}\right)$$

After the correction, a significant improvement in the μTPC angular resolution is observed.

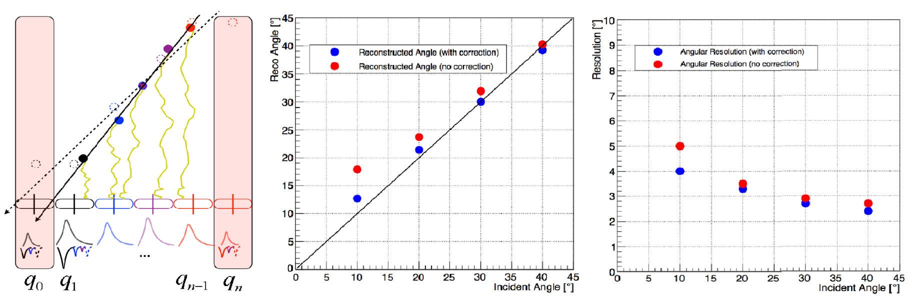

Figure 2: Left: sketch of the capacitative induction of the signals on neighbouring strips. Center: reconstructed angles before and after the correction. Right: angular resolution of a single MM chamber as a function of the beam incidence angle, before and after correction.

4.2 Spatial resolution

The spatial resolution has been studied exploiting both the charge centroid and the μTPC methods. It was measured using two MM chamber (specified by i and j indices) with the same orientation in respect to the beam direction and evaluating the distribution width of the following quantities:

- $\left(x^i_{centroid} - x^j_{centroid}\right)/\sqrt{2}$ for the centroid method,
- $\left(x^i_{half} - x^j_{half}\right)/\sqrt{2}$ for the μTPC method,

in which $x_{centroid}$ is the charge centroid X coordinate while x_{half} is the X coordinate of the track segment, reconstructed using uTPC, at half drift gap.

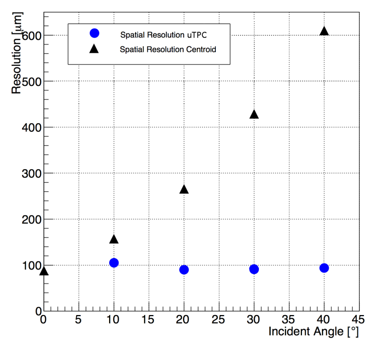

Figure 3: MM spatial resolution as a function of the beam incidence angle (results on July '12 CERN test beam data). In the NSW the typical angles of incidence are expected to be between $8° \div 35°$.

A double gaussian fit was performed in order to take into account the tails of the distribution [4] and the σ of the narrow gaussian has been used as indicator of the resolution, found to be better than 100 μm in the full angular range, as shown in Fig.3.

4.3 Micromegas inefficiency

The MM chamber inefficiency is obtained by tracking through all chambers but one and looking for missing hits in the test chamber. For this study, June '13 DESY test beam data have been used. The plot in Fig.4 (referred to a T chamber with $HV = 500\ V$ and $\theta = 0°$) shows that inefficiencies are mostly due to the pillars, where the mesh is held tensioned. Pillars have a diameter 300 μm and are spaced by 2.5 mm. For this study, three kinds of inefficiencies have been defined:

- **hardware inefficiency** $(1 - \epsilon_h) \rightarrow$ no hit in T3 chamber;
- **cluster inefficiency** $(1 - \epsilon_c) \rightarrow$ no cluster in T3 chamber;
- **software inefficiency** $(1 - \epsilon_s) \rightarrow$ no cluster within 10 σ from extrapolated position in T3 chamber.

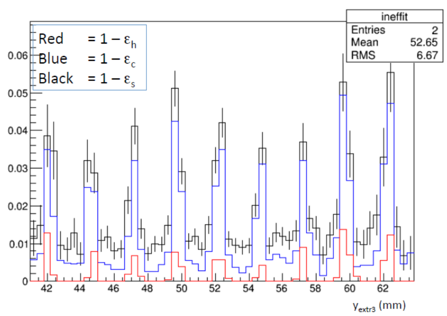

Figure 4: Inefficiencies as a function of the extrapolated position on T3 chamber.

- $1 - \epsilon_h = 0.19\%$
- $1 - \epsilon_c = 1.34\%$
- $1 - \epsilon_s = 1.95\%$

An average inefficiency less than 2% is observed for runs with tracks at $\theta = 0$, while an efficiency improvement is observed at larger angles.

References

1. The ATLAS Collaboration, New Small Wheel, Technical Design Report, CERN-LHCC-2013-006.

2. M.Iodice *on behalf of the MAMMA Collaboration*, Performance studie of MicroMegas for the ATLAS experiment, IOP Science - Journal of Instrumentation, **9**, 1-15, (2014).

3. C.Bini *on behalf of the MAMMA Collaboration*, Study of the performance of the Micromegas chambers for the ATLAS muon spectrometer upgrade, IOP Science - Journal of Instrumentation, **9**, 1-9, (2014).

4. M. Trovatelli, Performance studies on MicroMegas detector, Il Nuovo Cimento, Vol. 37 C, N. 1, (2014).